

Understanding the impact of space charge variations with UV- and water-aged epoxy alumina nanocomposites adopting pulsed electroacoustic techniques

Neelmani¹, Ramanujam Sarathi¹ ✉, Hisayuki Suematsu²

¹Department of Electrical Engineering, IIT Madras, Chennai 600 036, India

²Extreme Energy-Density Research Institute, Nagaoka University of Technology, Nagaoka 940-2188, Japan

✉ E-mail: rsarathi@iitm.ac.in

Published in Micro & Nano Letters; Received on 30th March 2020; Revised on 14th July 2020; Accepted on 3rd August 2020

Epoxy alumina nanocomposites were prepared to understand the space charge variations with ultra violet (UV)- and water-aged specimens. Addition of alumina nanofiller to epoxy resin had suppressed the space charge formation. A pulsed electroacoustic technique was employed to measure the space charge accumulation in epoxy–alumina nanocomposites. A marginal increase in space charge with enhanced electric field in the bulk volume of insulation was observed with UV- and water-aged nanocomposites. It was observed that 3 wt% sample showed better performance in all ageing conditions, which was confirmed through space charge studies and by the measurement of the dielectric parameters especially dielectric constant and $\tan(\delta)$.

1. Introduction: Polymeric insulators are widely used in the outdoor applications because of its high electrical performance, hydrophobic surface, and reduced installation cost, and among all polymeric insulators epoxy resin emerges as one of the best insulators. Electrical performance of epoxy resin can be enhanced by introducing different kinds of nanofillers to the base epoxy resins and alumina nanoparticles emerge to be the best one [1, 2]. Exposure of outdoor insulators to ultra violet (UV) irradiation has high impact on its electrical and insulating properties of insulators. UV radiation alters the molecular structure and leads to degradation of insulators [3]. Ning *et al.* studied the impact of UV irradiation with epoxy MgO nanocomposites on space charge accumulation studies. They have identified that higher wt% of MgO with epoxy resin can reduce the space charge accumulation. In addition, after 50 h of UV irradiation, the space charge enhancement gets stabilised [4].

In addition, the problem with the outdoor insulators is the diffusion of water into its bulk volume during rainy or humid weather conditions, which changes its bulk electrical properties, especially the dielectric constant and $\tan(\delta)$. Qiang *et al.* [5] studied the properties of epoxy silica nanocomposites on water absorption and have indicated that addition of nanosilica enhances the water absorption in its bulk volume.

Accumulation of space charge in the bulk of polymeric insulators alters its insulating properties and leads to electric breakdown of insulators. Space charge accumulation can cause the enhancement in the local electric field leading to the premature failure of insulating materials [6]. Recent studies show that incorporation of nanoparticles into the base polymer resin suppresses the space charge accumulation [7]. Hence, it is essential to understand the influence of alumina nanoparticles on the space charge accumulation behaviour of epoxy–alumina nanocomposites, and also the impact of UV radiation and water ageing on the space charge characteristics of epoxy–alumina nanocomposites. There are different techniques adopted for measuring the space charge (including thermal pulse, laser-intensity modulation, laser-induced pressure pulse, pressure wave propagation etc.) in the insulating material and each method has its own advantages and disadvantages. However, the pulsed electroacoustic (PEA) is one of the most reliable and promising techniques for space charge studies [8]. Hence, in this Letter, the PEA technique is used for space charge measurement.

Having known all the facts, a methodical experimental study was carried out to understand the impact of dielectric property variations

and space charge variations adopting the PEA technique, with UV- and water-aged epoxy–alumina nanocomposites.

2. Experimental studies

2.1. Sample preparation: In this Letter, epoxy–alumina nanocomposites were prepared using base epoxy resin (Araldite CY 205 in liquid, solvent-free, unmodified Bisphenol A epoxy purchased from HUNTSMAN) and alumina nanoparticles with purity of 99.9% and size of 20–30 nm (purchased from Richem international, USA). Fig. 1 shows the schematic representation for the preparation of epoxy–alumina nanocomposites. Moisture content in the alumina nanoparticles was removed by keeping it in oven at 150°C for 24 h. The dried alumina nanoparticles were uniformly dispersed in ethanol using high-frequency sonicator. The appropriate amount of epoxy was uniformly mixed with the alumina–ethanol solution using high-speed shear mixture operated at a speed of 4000 rpm for 6 h followed by high-frequency sonication process (for 1 h at 20 kHz). Later, appropriate amount of hardener (tri-ethylene tetra-amine purchased from HUNTSMAN) was added to the epoxy–alumina mixture and was degassed to remove air bubbles. At last, degassed mixture was poured in the mould of defined size and left for curing at room temperature, for 24 h. Epoxy nanocomposites were prepared using 0, 1, 3, and 5 wt% of alumina nanoparticles.

2.2. UV ageing and water ageing test: UV ageing process of epoxy–alumina nanocomposites was performed using xenon lamp of 600 W, 230 V (TRA-VITALUX) kept in UV chamber. This lamp produces the uniform flux and it covers the wavelength range of 200–400 nm. A distance of 20 cm was maintained between the samples and xenon lamp during the UV ageing process. UV ageing of epoxy–alumina nanocomposites was carried out for 150 and 300 h. Water ageing of samples was carried out using deionised water and the samples immersed into the deionised water were kept in oven at 90°C. The weight gained by the epoxy–alumina nanocomposites was continuously monitored and water ageing was continued till the saturation in the weight gained is achieved by all the samples.

2.3. Dielectric relaxation spectroscopy: Novo control broadband dielectric/impedance spectrometer (Alpha-A high performance frequency analyser) was employed to measure the dielectric

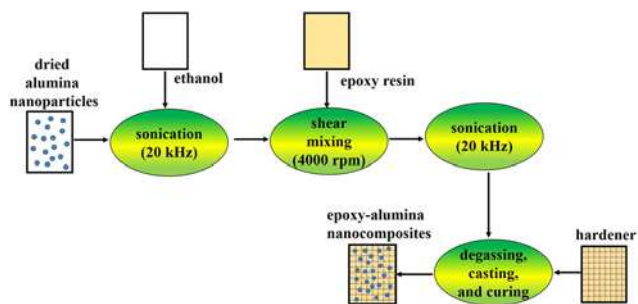


Fig. 1 Schematic representation for the preparation of epoxy-alumina nanocomposites

constant and $\tan(\delta)$ of the nanocomposites and these measurements were taken at the different frequencies in the range of 10^{-1} – 10^6 Hz.

2.4. Space charge measurement: In this Letter, the PEA technique was adopted for the measurement of space charge in the bulk of epoxy-alumina nanocomposites. Fig. 2 shows the schematic diagram of Techimp PEA space charge measurement setup. The PEA setup involves PEA flat cell, a variable DC source of 0–30 kV, a pulse generator of 0–500 V, a DC power supply of 18–24 V for the amplifiers in the cell and an oscilloscope (Tektronix, 350 MHz, 5 GS/s). The test sample dimension of $40 \times 40 \times 1.5$ mm was used for the space charge measurement. In this Letter, nanocomposites were stressed with an electric field of 14 kV/mm for 1 h (poling period) and depoling (voltage off) was done for another 1 h in order to deplete the space charge from nanocomposites. Poling and depoling were done for 1 h for all the samples.

3. Results and discussion

3.1. Dielectric response studies: Fig. 3 shows the dielectric constant and loss tangent at different frequencies for UV- and water-aged specimen. Dielectric properties of insulating materials are totally dependent on the presence of orientational dipoles into the materials and its tendency to orient along the external applied electric field [9]. In epoxy nanocomposites, weak covalent bonded molecular groups are present in the form of dipoles and their orientation changes on application of electric field leading to the variation in dielectric constant, at different frequencies. At lower frequencies, it is easy for the dipolar group to orient themselves along the external electric field causing higher value of dielectric constant. At higher frequencies, the dipolar group cannot respond to the fast varying electric field, as a result the decrement in the dielectric constant was observed for higher frequencies. Addition of alumina nanofiller enhanced the dielectric constant and $\tan(\delta)$ of the nanocomposites. Increment in $\tan(\delta)$ can be attributed to the presence

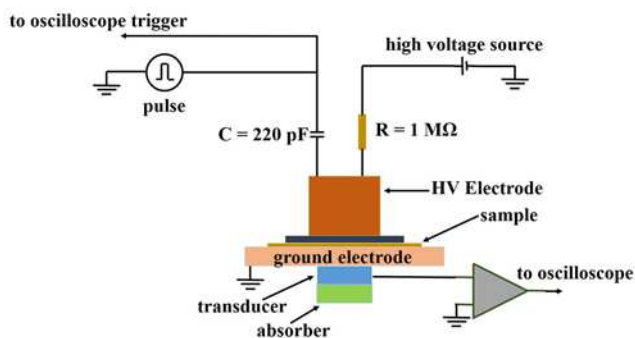


Fig. 2 Space charge measurement setup

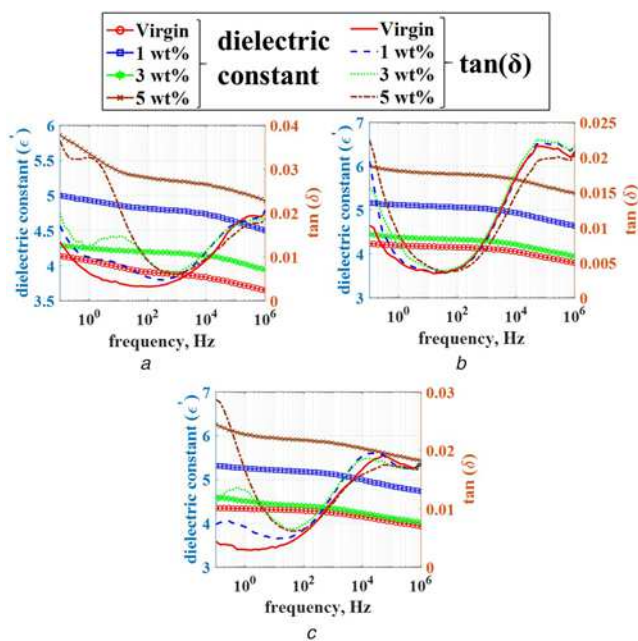


Fig. 3 Variation in dielectric constant and loss tangent at different frequencies for
a Unaged samples
b 300 h UV-aged samples
c Water-aged samples

of mobile charge carriers and the amount of these charge carriers is enhanced on the addition of nanofiller.

In the case of UV ageing process, different chain scission and crosslinking process result in formation of radicals and also can cause breakage of weak covalent bond [10]. These newly formed radicals and breaking of covalent bond aid the process of dipolar orientation resulting into the increment of dielectric constant compared to unaged samples. The $\tan(\delta)$ for UV-aged samples was found to be more than the unaged samples.

For water-aged samples, dielectric constant of all the samples was higher at all the frequencies as compared to unaged samples. The presence of water molecules in the samples loosens the weak covalent bond which enhances the movement of different dipolar groups resulting into the enhancement of dielectric constant. Qiang *et al.* studied the effect of water absorption on the dielectric properties of epoxy silica and boron nitride nanocomposites and observed that permittivity of nanocomposites is strongly affected by the water absorptions. They observed the increment in permittivity value for water absorbed epoxy silica nanocomposites [11]. In general, it is observed that the permittivity and $\tan(\delta)$ variation due to UV ageing and water ageing are observed to be minimum with 3 wt% alumina added epoxy resin. Admittedly, it is essential to understand the characteristic variation in the material due to ageing, through various physio-chemical diagnostic studies, which will be carried out at near future.

3.2. Space charge distribution: Fig. 4 shows the space charge profile for the unaged samples. Homocharges formation was observed near both the electrodes for all the samples and the amount of homocharges increased with the poling time. The presence of homocharges can be attributed to charge injection from the electrodes in the form of electrons and holes [12]. In the case of alumina-filled epoxy nanocomposites, a large amount of homocharges injection was observed. Homocharges formed near the anode start moving towards the cathode and near cathode less amount of homocharges were observed due to neutralisation with negative charges.

The characteristics of space charge profile formed with water-aged specimen and the UV-aged specimen were much similar and

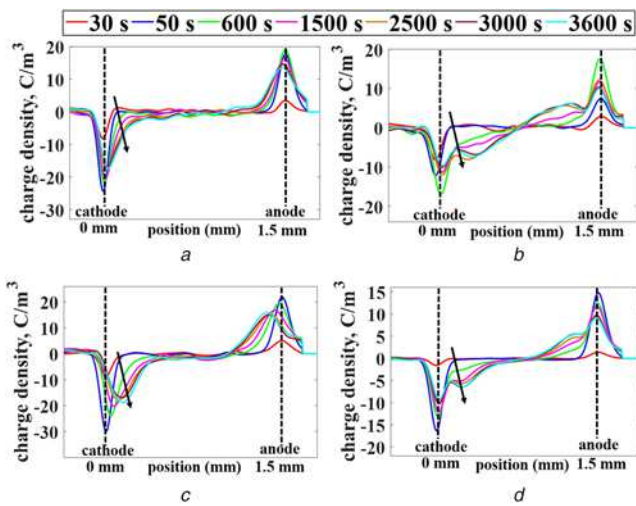


Fig. 4 Space charge profile during poling under the electric field of 14 kV/mm for
a Pure epoxy
b 1 wt% alumina-filled epoxy nanocomposites
c 3 wt% alumina-filled epoxy nanocomposites
d 5 wt% alumina-filled epoxy nanocomposites

the analysis was carried out with the electric field of 14 kV/mm. For 150 h of UV-aged samples, the homocharges formation was observed near both the electrodes for all the samples. This homocharges formation seems to be higher for epoxy–alumina nanocomposites compared to unaged nanocomposites. For 300 h UV-aged samples, the heterocharges formation was observed in the vicinity of cathode and anode. This heterocharges formation could be due to radiation causing different internal processes, such as chain scission, crosslinking, gas bubble formation, and formation of new radicals, and also due to the presence of dominant charge carriers. Ning *et al.* [13] have indicated the possibility of formation of molecular structure variation causing charge trap sites. Han *et al.* [14] have clearly indicated that the UV irradiation can break some of the chemical bonds of the epoxy resin, causing ageing and degradation of the resin. With 3 wt% of alumina nanofiller, less heterocharges formation near cathode was observed and this could be due to neutralisation phenomenon occurred near the cathode [15].

The PEA analysis of water-aged nanocomposites indicated the heterocharges formation near the electrodes. This heterocharges formation could be due to the presence of some impurities and presence of water molecules that produce ions (OH^- , H_3O^+). These ions will add up the heterocharges formation. Increase in the magnitude of heterocharges near cathode was more, which indicates the presence of dominant positive charge due to water on surface layer of the specimens.

Fig. 5 shows the space charge profile of the epoxy–alumina nanocomposites specimen during 1 h of depoling period. Heterocharges formation was observed in all the nanocomposites and in epoxy samples. Addition of 1 and 3 wt% of alumina nanofiller decreases the magnitude of heterocharges formed during the depoling period. Similarly, heterocharges formation was observed in all the UV- and water-aged samples, and after 1 h of depoling period almost all the space charge decayed out in the specimen.

Average space charge density accumulated in the bulk of nanocomposites can be estimated using the following equation:

$$q_s(E, t) = \frac{1}{X_1 - X_0} \int_{X_0}^{X_1} \text{Abs}[q_p(X, t)] dX \quad (1)$$

where X_0 and X_1 are the electrode positions (charges induced at the electrodes are not taken into the consideration), E is the applied

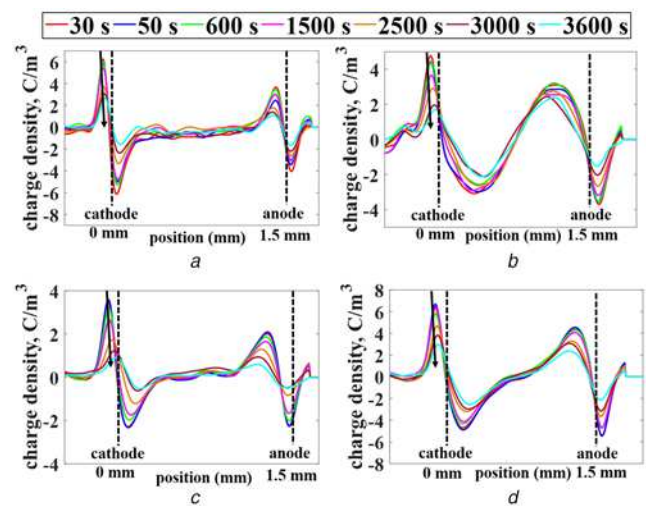


Fig. 5 Space charge profile during depoling for
a Pure epoxy
b 1 wt% alumina-filled epoxy nanocomposites
c 3 wt% alumina-filled epoxy nanocomposites
d 5 wt% alumina-filled epoxy nanocomposites

electric field, t is the poling and depoling time, and $\text{Abs}[q_p(X, t)]$ is the absolute value of the charge profile.

Fig. 6 shows the space charge accumulation process during the poling period for unaged and aged samples of epoxy–alumina nanocomposites. It was realised that the charge accumulation process appears to be continuing with epoxy–alumina nanocomposites, irrespective of percentage of alumina in epoxy resin. The accumulation of space charge in the insulating material is highly dependent on the charge injection and transport processes. Introduction of nanofiller in base material causes trap levels of different energies, which alters the charge trap distribution in the materials, resulting into the variation of space charge accumulation [16]. With 1 wt% of alumina nanofiller loading (lower wt% of loading), shallow traps have been introduced into the materials resulting into the increment of apparent mobility of the charge

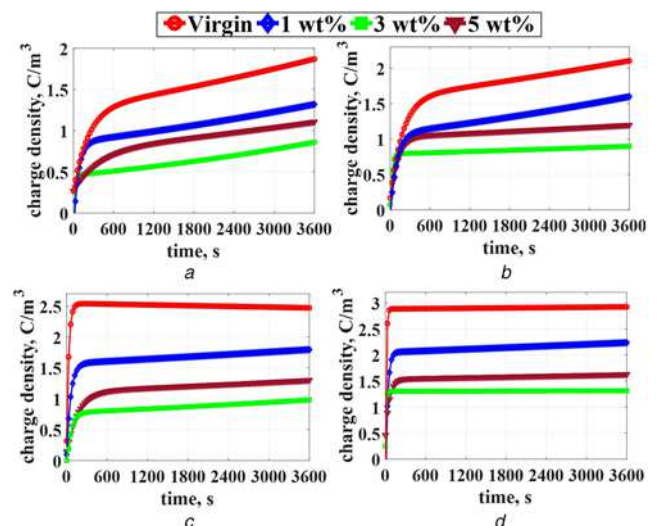


Fig. 6 Space charge density in the bulk of pure epoxy and different wt% of alumina-filled nanocomposites under the electric field of 14 kV/mm during poling for
a Unaged samples
b 150 h UV-aged samples
c 300 h UV-aged samples
d Water-aged samples

carriers, so less space charge accumulation in the bulk volume of insulation [17]. On further loading of alumina nanofiller (3 wt%), inter-filler distance apparently reduces which results into the overlap of shallow trap bands. In the process, trap energy level between these bands decreases which further decreases the apparent mobility resulting into less space charge accumulation than 1 wt% alumina added nanocomposites [17, 18]. The shallow traps correspond to the weak interfacial binding force. At higher wt% of alumina nanofiller, interfacial binding force will be more strong, which results in increment in trap energy level, which means more deep traps and less shallow traps introduced. This increment in the energy level at the interface blocks the charge carriers, resulting in increased space charge accumulation in the 5 wt% sample [16, 19]. Compared to unaged samples, different hours of UV-aged and water-aged samples accumulated more charges in its bulk. As indicated earlier, during UV ageing process, different

internal processes such as chain scission, crosslinking, gas bubble formation, and formation of new radicals can form. These new crosslinked bonds and radicals act as a trap for charge carriers enhancing space charge density in the bulk volume of the insulating material.

In the case of the water-aged samples, water occupies the inter-molecular space which was previously occupied by some atmospheric gas or some small voids, resulting into the increment of sample weight without any change in its volume. Neelmani *et al.* have carried out water diffusion in epoxy nanocomposites and have indicated that water uptake is reduced on addition of alumina and 5 wt% sample showed lowest weight gain. Diffusion coefficient of water into the epoxy nanocomposites was calculated and has showed decreasing value with increase of alumina content in epoxy resin [20]. The time to reach saturated weight and saturated % wt gain by the samples is shown in Table 1. The presence of nanofillers acts as a barrier in diffusion of water to the bulk volume of the epoxy–alumina nanocomposites. Introduction of nanoparticles produces strong interfacial bonding between matrix and nanoparticles. As a result, in the case of nanocomposites, water diffuses and gets concentrated at the interfacial region around the nanoparticles. At higher wt% these interfacial region overlaps, as result availability of interfacial region decreases, leading to reduction in water uptake [16].

During water ageing, the diffused water tries to loosen the polymer chain and damage the interfacial bonding resulting it to be the point of local site for charge to get trapped enhancing space charge density in the bulk volume of water-aged epoxy nanocomposites. Pure epoxy sample accumulates more space charge compared to epoxy–alumina nanocomposites. Water uptake was less in case of nanocomposites, so less ionised charges, as a result less accumulation of space charge. With 1 and 3 wt% sample, gradual reduction in space charge was observed. In case of 5 wt% of alumina nanofiller loaded epoxy nanocomposites, due to overlapping of interfacial regions, number of shallow traps decreased and deep traps increased, resulting into a marginal increase in space charge.

On water/UV ageing, it was observed that the charge density in the bulk volume of insulation has attained saturation in a short period of time and was observed to occur early with the water-aged specimen.

Fig. 7 shows the space charge characteristics during the depoling period for unaged and aged epoxy–alumina nanocomposites. Increment in wt% of alumina nanofiller decreases the space charge accumulation and increases the decay rate of charge accumulated during depoling period due to the presence of shallow traps. Decay of space charge density on removal of applied electric field can be approximated as exponential decay:

$$Q(t) = Q_0 * e^{-\alpha t} \quad (2)$$

where Q_0 is the initial space charge and α is the decay rate.

The initial space charge and decay rate for unaged and UV/water-aged samples were tabulated in Table 2. The decay rate increased

Table 1 Parameters of water-aged samples

Samples	Time to reach saturation, h	Saturated weight, %
virgin	76.8	4.801
1 wt%	67.2	4.381
3 wt%	58	4.3
5 wt%	45	3.908

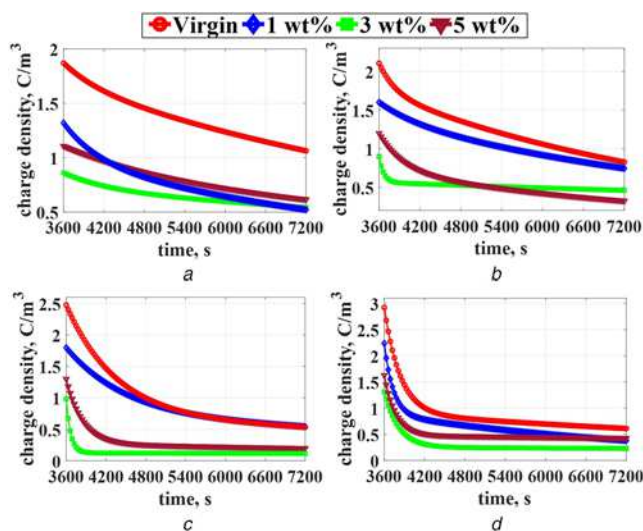


Fig. 7 Decay of space charge density from the bulk of pure epoxy and different wt% of alumina-filled nanocomposites under the electric field of 14 kV/mm during depoling for
a Unaged samples
b 150 h UV-aged samples
c 300 h UV-aged samples
d Water-aged samples

Table 2 Decay rate of the space charge formed at the 14 kV/mm electric field in all unaged, and UV- and water-aged samples

Samples, wt%	Initial space charge, Q_0 , C/m ³				Decay rate (α)			
	A	B	C	D	A	B	C	D
0	1.87	2.1059	2.4743	2.9207	0.001914	0.001654	0.001345	0.003224
1	1.319	1.5990	1.7960	2.2350	0.002927	0.001786	0.001524	0.00397
3	0.86	0.8977	0.9824	1.31	0.0049	0.00368	0.00354	0.00543
5	1.107	1.1983	1.2990	1.62	0.00371	0.002839	0.002312	0.00425

A: unaged, B: 150 h UV aged, C: 300 h UV aged, D: water aged.

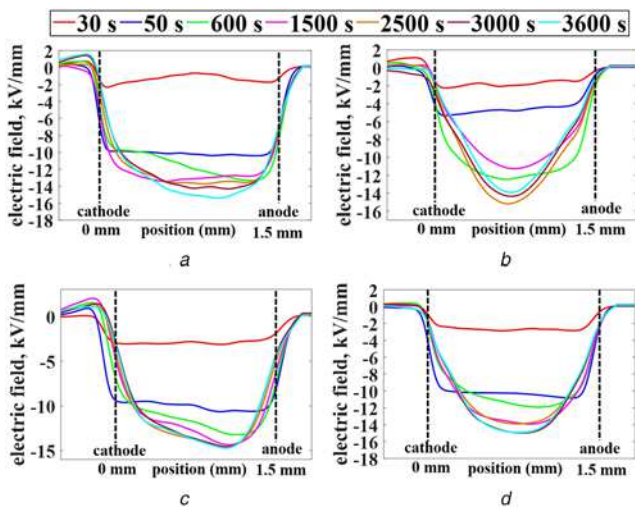


Fig. 8 Electric field distribution under the electric field of 14 kV/mm in
a Pure epoxy
b 1 wt% alumina-filled epoxy nanocomposites
c 3 wt% alumina-filled epoxy nanocomposites
d 5 wt% alumina-filled epoxy nanocomposites

Table 3 Electric field enhancement factor for unaged, and UV- and water-aged samples under the applied electric field of 14 kV/mm

Samples, wt%	% Electric field enhancement (E)			
	Unaged	150 h UV aged	300 h UV aged	Water aged
0	9.786	13.07	16.35	87.12
1	8.5	42.14	7.143	45.57
3	4.93	5.4285	16.42	29.5
5	6.57	27	10.35	30.21

for the alumina-filled epoxy nanocomposites and it was high for the 3 wt% filled alumina nanocomposites. In the case of UV irradiated samples, decay rate decreased and initial charge density increased for all the samples on increasing the number of UV hours ageing and this was due to the trapping of charges because of the formation of new radicals and crosslinking phenomenon.

For water-aged sample, decay rate during depoling time was found to be high compared to unaged samples and UV-aged samples irrespective of wt% of alumina nanofiller in epoxy resin. The cause for it could be due to reduction in the average distance between the trap sites, as a result charge carrier can easily move from one site to another site, enhancing the conductivity of the medium and also the overlapped water shell around nanofiller provides continuous path for charge carriers to travel through, leading to reduced decay rate. Lewis *et al.* [21] observed similar phenomena with low density polyethylene (LDPE) nanocomposites.

3.3. Electric field enhancement: Fig. 8 shows the electric field distribution in the pure epoxy and alumina-filled epoxy nanocomposites under the applied electric field of 14 kV/mm. Field enhancement was observed in the middle of epoxy–alumina nanocomposite samples and which could be due to the movement of charges from their respective electrodes. Similar characteristics were observed with UV-irradiated samples and water-aged samples. Field distortion and field enhancement were observed with the aged specimens.

Accumulation of space charge in the bulk of the nanocomposites changes the applied electric field and increases the electric field distribution in the nanocomposites. The percentage enhancement

factor (E) can be calculated using the following equation:

$$E = \frac{E_m - E_{\text{appl}}}{E_{\text{appl}}} \times 100 \quad (3)$$

where E_m is the maximum electric field in the sample at the end of 1 h of poling period and E_{appl} is the applied electric field. Percentage enhancement factor was calculated for unaged and aged samples and was tabulated in Table 3. It was observed that water-aged samples showed maximum electric field enhancement compared to UV-aged and unaged samples. It was also observed that 3 wt% sample showed better performance compared to other samples in all ageing conditions.

4. Conclusion: In general, addition of alumina nanoparticles suppressed the space charge formation in the bulk volume of epoxy–alumina nanocomposites. UV- and water-aged samples accumulated higher space charge compared to unaged samples. Water-aged samples showed highest decay rate of space charge during depoling period, due to the reduction in the average distance between the trap sites. It was observed that water-aged samples showed maximum electric field enhancement compared to UV-aged and unaged samples. It was observed that 3 wt% sample showed better performance in all ageing conditions, which was confirmed through space charge studies and by measure of dielectric parameters especially dielectric constant and $\tan(\delta)$.

5. Acknowledgments: The author (R.S.) wishes to thank Central Power Research Institute, Bangalore, India for sponsoring the project (NPP/2016/TR /1/ 27042016) on nanocomposites.

6 References

- [1] Tanaka T., Imai T.: ‘Advanced nanodielectrics: fundamentals and applications’ (CRC Press, USA, 2017)
- [2] Chen Y., Zhang D., Wu X., *ET AL.*: ‘Epoxy/ α -alumina nanocomposite with high electrical insulation performance’, *Prog. Nat. Sci. Mater. Int.*, 2017, **27**, (5), pp. 574–581
- [3] Peng D., Qin W., Wua X.: ‘A study on resistance to ultraviolet radiation of POSS-TiO₂/epoxy nanocomposites’, *Acta Astronaut.*, 2015, **111**, pp. 84–88
- [4] Ning X., Xiang Z., Peng Z., *ET AL.*: ‘Effect of UV ageing on space charge characteristics of epoxy resin and its nanocomposites’. IEEE Int. Conf. on Solid Dielectrics, Bologna, Italy, 2013, pp. 784–787
- [5] Qiang D., Chen G., Andritsch T.: ‘Influence of water absorption on dielectric properties of epoxy SiO₂ and BN nanocomposites’. Annual Report Conf. on Electrical Insulation and Dielectric Phenomena, Ann Arbor, MI, USA, 2015, pp. 439–442
- [6] Zhou C., Chen G.: ‘Space charge and AC electrical breakdown strength in polyethylene’, *IEEE Trans. Dielectr. Electr. Insul.*, 2017, **24**, (1), pp. 559–566
- [7] Wang Y.N., Wang Y.L., Wu J.D., *ET AL.*: ‘Research progress on space charge measurement and space charge characteristics of nanodielectrics’, *IET Nanodielectr.*, 2018, **1**, (3), pp. 114–121
- [8] Ahmed N.H., Srinivas N.N.: ‘Review of space charge measurements in dielectrics’, *IEEE Trans. Dielectr. Electr. Insul.*, 1997, **4**, (5), pp. 644–656
- [9] Singha S., Thomas M.J.: ‘Dielectric properties of epoxy nanocomposites’, *IEEE Trans. Dielectr. Electr. Insul.*, 2008, **15**, (1), pp. 12–23
- [10] Petersen E.J., Lam T., Gorham J.M., *ET AL.*: ‘Methods to assess the impact of UV irradiation on the surface chemistry and structure of multiwall carbon nanotube epoxy nanocomposites’, *Carbon*, 2014, **69**, pp. 194–205
- [11] Qiang D., Wang Y., Chen G., *ET AL.*: ‘Dielectric properties of epoxy silica and boron nitride nanocomposites and moisture/temperature influences’, *IET Nanodielectr.*, 2018, **1**, (1), pp. 48–59
- [12] Li Y., Tian M., Lei Z., *ET AL.*: ‘Effect of nano-silica on dielectric properties and space charge behavior of epoxy resin under temperature gradient’, *J Phys. D: Appl. Phys.*, 2018, **51**, (12), pp. 1–12
- [13] Ning X., Xiang Z., Peng Z., *ET AL.*: ‘Effect of UV ageing on space charge characteristics of epoxy resin and its nanocomposites’. 2013 IEEE Int. Conf. Solid Dielectr., Bologna, Italy, 2013, pp. 784–787

- [14] Han W.H., Xu Z.H., Wang X.Y., *ET AL.*: 'Mechanism of organic coating damage induced by ultraviolet radiation and its prevention measures', *Petrol. Eng. Constr.*, 2007, **33**, pp. 18–20
- [15] Qiang D., Wang Y., Wang X., *ET AL.*: 'The effect of filler loading ratios and moisture on DC conductivity and space charge behaviour of SiO₂ and hBN filled epoxy nanocomposites', *J. Phys. D. Appl. Phys.*, 2019, **52**, pp. 1–16
- [16] Lewis T.J.: 'Interfaces are the dominant feature of dielectrics at the nanometric level', *IEEE Trans. Dielectr. Electr. Insul.*, 2004, **11**, pp. 739–753
- [17] Wu J., Yin Y., Lan L., *ET AL.*: 'Space charge trapping and conduction in low-density polyethylene/silica nanocomposite', *Jpn. J. Appl. Phys.*, 2012, **51**, p. 041602
- [18] Tanaka T., Kozako M., Fuse N., *ET AL.*: 'Proposal of a multi-core model for polymer nanocomposite dielectrics', *IEEE Trans. Dielectr. Electr. Insul.*, 2005, **12**, (4), pp. 669–681
- [19] Montanari G.C., Fabiani D., Dissado L.A.: 'A new conduction phenomenon observed in polyethylene and epoxy resin: ultra-fast soliton conduction', *J. Polym. Sci., Part B*, 2011, **49**, (16), pp. 1173–1182
- [20] Neelmani, Velmurugan R., Jayaganthan R., *ET AL.*: 'Investigation of surface strain by digital image correlation and charge trap characteristics of epoxy alumina nanocomposites', *Nano Express*, 2020, **1**, p. 010043
- [21] Lewis T.J.: 'Polyethylene under electrical stress', *IEEE Trans. Dielectr. Electr. Insul.*, 2002, **9**, (5), pp. 717–729